Dip-correction for coherence-based migration velocity analysis

R. Biloti and J. Schleicher

email: *js@ime.unicamp.br*

keywords: *migration velocity analysis, coherence, velocity moveout*

ABSTRACT

Migration velocity analysis (MVA) is a seismic processing step that aims at translating the velocity information that is contained in the residual moveout in an image gather after migration with an erroneous velocity model into velocity updates. In this paper, we extend the original coherence-based MVA approach to dipping reflectors. We devise a new MVA technique, where the reflector dip is treated as an additional search parameter that is to be detected together with the velocity updating factor. Both parameters are searched-for simultaneously by the application of two-parameter search techniques. The search is carried out by determining trial curves as a function of the search parameters and stacking the migrated data along these curves. The highest coherence determines the best-fitting curve and thus the optimal, i.e., best-possible, parameter pair. A numerical example demonstrates that the additional search parameter can indeed be helpful to improve the quality of the velocity updates.

INTRODUCTION

Migration velocity analysis (MVA) is a seismic processing step that exploits the redundancy of seismic data to improve an a-priori velocity model. The basic idea is to use the velocity information that is contained in the residual moveout in an image gather, i.e., a CMP gather of the prestack migrated image cube, after migration with an erroneous velocity model (Yilmaz and Chambers, 1984). MVA aims at translating this residual moveout into velocity updates (Al-Yahya, 1989; Fowler, 1995). Of course, the process can be applied repetitiously, thus generating a loop between migration, MVA, and velocity updates, which is terminated when the residual moveout is sufficiently flattened.

The initial concepts soon led to a wide range of more sophisticated techniques. One of the first developments was the picking-free differential semblance optimization (DSO) of Symes and Carazzone (1991). Lafond and Levander (1993) generalized Al-Yahya's method to arbitrary heterogenous media, based on ray tracing rather than an analytical formula for the residual moveout. Bradford and Sawyer (2002) suggested three implementations of MVA methods that progress from relatively simple to relatively complex and computationally intensive. Further developments include a residual moveout analysis on a sparse grid of common midpoints points (CMPs) (Audebert et al., 1998; Woodward et al., 1998) or, more recently, along a fine grid following horizons (see, e.g., Billette et al., 2002). In parallel, other algorithms, based on picking of either continuous (Liu, 1997) or locally coherent (Chauris et al., 2002a,b) events were suggested. A residual-migration wave-equation tomographic technique has been proposed by Biondi and Sava (1999). The efficiency and accuracy of these various migration-based methods strongly depend on the density of points where the analysis is carried out (Billette et al., 2003).

In this paper, we follow the lines of the coherence-based approach of Al-Yahya (1989). In other words, we propose a semblance analysis along certain stacking curves within the data. This approach has the advantage that no picking is needed. We extend the method of Al-Yahya (1989), which was restricted to horizontal reflectors, to dipping reflectors. A first attempt in this respect was undertaken by Lee and Zhang (1992) using near-offset and small-dip approximations. Here, we keep the assumption of small dips ($< 45^\circ$) but drop the restriction to small offsets.

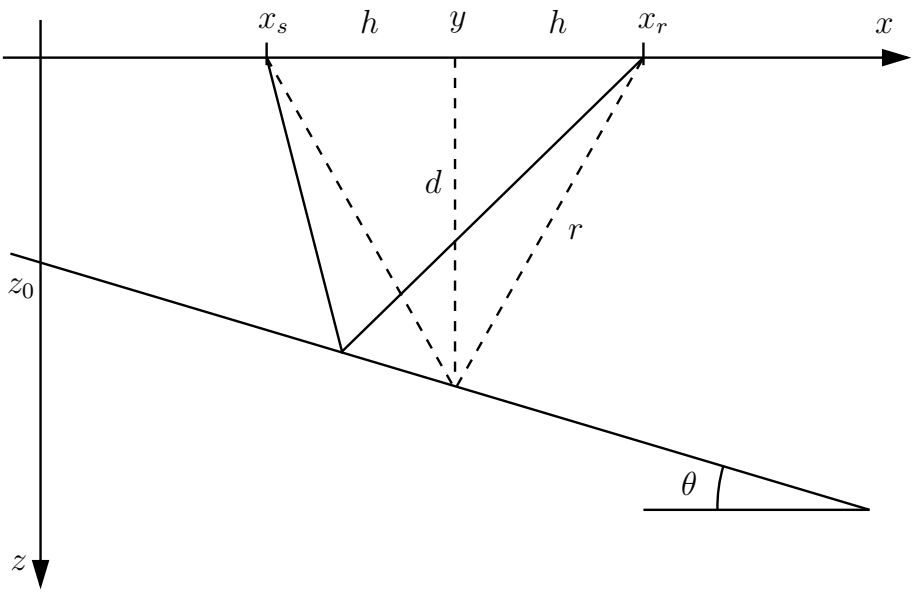

Figure 1: Reflector and acquisition geometry.

We devise a new MVA technique, where the reflector dip is treated as an additional search parameter which is to be detected together with the velocity updating factor. Both parameters are searched-for simultaneously by the application of techniques that have been developed in connection with the common-reflection-surface (CRS) stack (Biloti et al., 2002). Like for that method, the search is carried out by determining trial curves as a function of the search parameters and stacking the migrated data along these curves. The highest coherence determines the best-fitting curve and thus the optimal, i.e., best-possible, parameter pair.

DIPPING REFLECTOR

As a basis for the stacking technique, we need a theoretical expression for the position of a migrated reflector image as a function of the (wrong) migration velocity. For this purpose, we consider a dipping reflector with dip $m = \tan\theta$, where θ is the dip angle. The depth z of this reflector at a horizontal position x is thus described by the formula $z = mx + z_0$, where z_0 is the depth of the reflector vertically below the coordinate origin (see Figure 1). We consider this reflector $z = mx + z_0$ to be buried in a homogeneous medium with true velocity v.

Next, we consider a 2D seismic experiment being carried out over this medium along the x-axis. Sources and receivers are positioned at points $x_s = y - h$ and $x_r = y + h$, where y and h are the (varying) midpoint and half-offset coordinates (see again Figure 1). Then, the traveltime surface of the reflector in the data cube will be given by an expression of the form

$$t_{\text{ref}} = \frac{1}{v}\left(\sqrt{(x-y+h)^2+(mx+z_0)^2} + \sqrt{(x-y-h)^2+(mx+z_0)^2}\right) , \tag{1}$$

where x denotes the horizontal coordinate of the reflection point. The actual traveltime can be determined by applying Fermat's principle. It says that of all the traveltimes described by the above equation, actually only those will be observed that are stationary. Thus, by setting the derivative of equation (1) with respect to x equal to zero, the reflection points can be determined as a function of y and h. We have

$$\frac{\partial t_{\text{ref}}}{\partial x} = \frac{1}{v}\left(\frac{(x-y+h)+m(mx+z_0)}{\sqrt{(x-y+h)^2+(mx+z_0)^2}} + \frac{(x-y-h)+m(mx+z_0)}{\sqrt{(x-y-h)^2+(mx+z_0)^2}}\right) = 0 , \tag{2}$$

which can be solved for x to yield

$$x = \frac{(my + z_0)(y - mz_0) - mh^2}{(1 + m^2)(my + z_0)} \ . \tag{3}$$

Substitution of this result back in equation (1) yields, after some tedious algebraic manipulations, the final expression for the traveltime of a dipping reflector as a function of y and h,

$$t_{\text{ref}} = \frac{2}{v}\sqrt{\frac{h^2 + (my + z_0)^2}{1 + m^2}} \ . \tag{4}$$

To simplify the expressions below, we introduce the following notations. The depth d of the reflector point vertically below the midpoint y (see Figure 1) is given by

$$d = my + z_0, \tag{5}$$

and the distance between this reflector point and source or receiver is

$$r = \sqrt{d^2 + h^2} \ . \tag{6}$$

Moreover, we will use the factor

$$\mu = \sqrt{1 + m^2} = 1/\cos\theta \ . \tag{7}$$

With these notations, the horizontal coordinate (3) of the reflection point can be written as

$$x = \frac{d(d - \mu^2 z_0) - m^2 h^2}{m\mu^2 d}, \tag{8}$$

and the traveltime (4) takes the form

$$t_{\text{ref}} = \frac{2}{v}\,\frac{r}{\mu} = \frac{2}{v}\,r\cos\theta \ . \tag{9}$$

Equation (9) can be alternatively obtained from simple algebraic manipulations on the expression of Levin (1971).

REFLECTOR IMAGE

The reflection event located at the traveltime (9) in the data is now to be migrated using the (wrong) migration velocity v_m. Its position in a common-offset time-migrated section can be constructed as the envelope of the common-offset isochrons for all points (y, t_{ref}) in the data. Any of these isochrons is described by the lower half-ellipse

$$t(x; y, h) = \frac{2b}{v_m}\sqrt{1 - \frac{(x - y)^2}{a^2}} \ , \tag{10}$$

where t is the vertical time $t = 2z/v_m$ and where the semi-axes are given by $a = v_m t_{\text{ref}}/2$ and $b = \sqrt{a^2 - h^2}$. Here, x describes the horizontal coordinate of the image to be constructed. Since we are interested in the position of the image in an image gather, i.e., for a constant x, we can assume without loss of generality that the coordinate origin is located at the position of the present image gather, i.e., $x = 0$. Then, z_0 has the meaning of the true depth of the reflector at the considered image point.

Upon substitution of formula (4) for t_{ref} in equation (10), the family of isochrons reads

$$t(0; y, h) = \frac{2}{v_m}\,\frac{QR}{\gamma\mu r} \ , \tag{11}$$

where we have introduced the notations

$$Q = \sqrt{r^2\gamma^2 - \mu^2 y^2} \ , \tag{12}$$

$$R = \sqrt{r^2\gamma^2 - \mu^2 h^2} \ , \tag{13}$$

and where γ is the ratio between the migration and true medium velocities as defined by Al-Yahya (1989), i.e.,

$$\gamma = v_m/v \ . \tag{14}$$

As mentioned above, the reflector image is given by the envelope of this family of isochrons. The envelope can be computed again by setting the derivative of formula (11) with respect to y equal to zero, solving the resulting equation for y, and substituting this result in equation (11). In this way, the envelope condition reads

$$\frac{dt}{dy} = \frac{2}{v_m} \frac{\gamma^2 mdQ^2r^2 + R^2r^2(md - \mu^2 y) - Q^2R^2md}{\gamma\mu QRr^3} = 0 \ . \tag{15}$$

Unfortunately, this expression cannot be solved for y. We therefore have to look for an approximate envelope. For this purpose, we use the Taylor series up to third order in m instead of the true derivative (15). Consequently, all following formulas are valid if $m^3 \ll 1$, that is, for reflector dips up to about 30 degrees. Since the resulting Taylor series is quite large, we refrain from stating it here. It can be solved for y to yield, up to third order in m,

$$y \approx \gamma^4(h^2 + z_0^2) z_0 \frac{m}{q} \left[1 + \left(\gamma^2 q^2 + 2h^2 q - \gamma^2 z_0^2 (q + 3\gamma^2 h^2)\right) \frac{m^2}{q^2}\right] \ . \tag{16}$$

Here, we have introduced yet another abbreviating notation, this one being

$$q = (\gamma^2 - 1)h^2 + \gamma^2 z_0^2 \ . \tag{17}$$

Instead of developing equation (15) into a Taylor series with respect to m, i.e., for small dips, one could conceive of other possible approximations, such as small offsets (i.e., $h/z_0 \ll 1$), midpoints close to the considered image point (i.e., $y/z_0 \ll 1$), or even velocity ratios close to unity (i.e., $\gamma - 1 \ll 1$). Unfortunately, none of these Taylor series could be solved for the stationary value of y.

Substituting the stationary value (16) back in equation (11) yields the approximate position of the reflector image in the image gather as a function of half-offset h,

$$t_{\text{ig}}(h) \approx \frac{2}{v_m}\sqrt{q} + (1 - \gamma^2)\gamma^2 \frac{(h^2 + z_0^2)(h^2 - \gamma^2 z_0^2)}{v_m \sqrt{q^3}} \, m^2 \ , \tag{18}$$

again up to third order in m.

Of course, the depth z_0 of the reflector at the image point is unknown at this stage. It has to be replaced by its vertical time coordinate, i.e, $z_0 = vt_0/2 = v_m t_0/2\gamma$. The final expression for the position of the reflector image in the image gather reads thus

$$t_{\text{ig}}(h) \approx \tau + (1 - \gamma^2) \frac{(4\gamma^2 h^2 + v_m^2 t_0^2)(4h^2 - v_m^2 t_0^2)}{2v_m^4 \tau^3} \, m^2 \ , \tag{19}$$

where

$$\tau = \sqrt{t_0^2 + (\gamma^2 - 1)4h^2/v_m^2} \ . \tag{20}$$

We immediately observe that equation (20) is exactly Al-Yahya's expression for the image position of a horizontal reflector. Note that the additional factor 4 in the last term under the square root is due to the fact that Al-Yahya (1989) considers a migration slowness that corresponds to twice the medium slowness, i.e., his w_m relates to v_m as $w_m = 2/v_m$. Since Al-Yahya's expression is the first term of formula (19), we can interpret its second term as a dip-correction to Al-Yahya's formula. We stress that equation (19) is a third-order approximation in m. In other words, the first and third-order terms in m are zero. Therefore, the image gather contains no information about the sign of m, i.e., of the direction of the dip.

There are two important conclusions to be drawn from the second term in expression (19). Firstly, the proportionality factor $1 - \gamma^2$ confirms Al-Yahya's observation that the dip dependence of the reflector image position decreases as the migration velocity v_m approaches the true medium velocity v. Secondly, the equality at zero offset between t_{ig} and t_0, which Al-Yahya (1989) observed for horizontal reflectors, is no longer true for dipping reflectors. For zero offset, equation (19) reduces to

$$t_{\text{ig}}(0) \approx t_0 + (\gamma^2 - 1)t_0 m^2/2 \ . \tag{21}$$

This equation describes the well-known fact that a nonzero reflector dip causes the zero-offset image of the reflector to shift downwards, if the migration velocity is too high, and upwards, if the migration velocity is too low.

SEARCH TECHNIQUE

As suggested by Al-Yahya (1989) for its first term, we use equation (19) to carry out coherence analyses along trial lines defined by this equation. However, instead of searching for a single parameter γ for each t_0, we search for two of them, being γ and m. While γ, as before, is meant to determine an estimate for the true medium velocity from the migration velocity as

$$v_{\text{est}} = v_m/\gamma \ , \tag{22}$$

the main role of the second parameter m is to stabilize the search and get better estimates for γ in situations with dipping interfaces and/or where the first guess for v_m was quite bad. The actual values of m can be useful at the interpretation stage.

To determine the optimal values for γ and m, a biparametrical search has to be carried out. To make this bidimensional search computationally feasible, we need starting values for both parameters as close as possible to their optimal values. To determine these starting values, we first search one-dimensionally for each of them independently with the following strategy.

We remind that Al-Yahya's formula, which is accurate up to first order in m, depends only on γ. Only the second-order term of the proposed formula depends on both parameters, γ and m. This means that the velocity parameter γ plays a more important role than the dip parameter m. This observation suggests that the one-dimensional search for γ should precede the one for m.

Since our dip-correction was derived from a Taylor expansion for small m, the first stage of the search is to look for a value of γ that maximizes the coherence measure with m set to zero. In other words, the starting value for γ is obtained by a search using Al-Yahya's formula only. Once an initial estimate for γ has been found, a second one-dimensional search is performed with fixed γ to obtain an approximation for m. This procedure is only intended to obtain rough estimates for these two parameters, which serve as starting values for the subsequent bidimensional search. Finally, a derivative-free optimization method (Kolda et al., 2003) is employed to obtain the best possible values for γ and m simultaneously.

The described procedure follows the same search technique successfully employed to simultaneously obtain the three traveltime attributes of the Common-Reflection-Surface (CRS) stack (Birgin et al., 1999). Note that in the present application, the bidimensional search technique is even more advantageous than in the case of the CRS stack, where the search for the second and third parameters turned out to be quite time consuming. In the present application, the search for the additional parameter m (instead of looking only for γ) has a small impact on computation time.

NUMERICAL EXAMPLE

In this section, we demonstrate the application of the dip-corrected migration velocity analysis to a synthetic data set. The depth model is depicted in Figure 2. It consists of two half-spaces separated by a single reflector, which has horizontal segments at the left and right sides of the model at depths of 1.2 km and 0.5 km, respectively. These two horizontal parts are smoothly connected by a dipping reflector segment with a dip angle of 15 degrees. The wave speed is 2 km/s above the reflector and 3 km/s below it.

Synthetic seismic data have been generated by an implementation of modeling by demigration (Santos et al., 2000). For the numerical experiment, 281 sources where simulated at every 25 m along the seismic profile between coordinates $x = -1000$ m and $x = 6000$ m with 241 source-receiver offsets at every 25 m from 0 m up to 6000 m. These data have been migrated with the incorrect migration velocity of 3.5 km/s. On the resulting image gathers, coherence-based migration velocity analysis has been applied using Al-Yahya's original traveltime formula (20) and our dip corrected one, equation (19). Figure 3 shows a typical image gather at a migrated CMP at the horizontal position $x = 3500$ m, that is, located above the dipping part of the reflector. Note the strong moveout due to the way too high migration velocity. Also shown in Figure 3 are the predicted positions of the migrated reflector as determined by equations (19) and (20) using the correct values for γ and m. We observe a much better coincidence of the dip-corrected formula with the actual position than Al-Yahya's original formula.

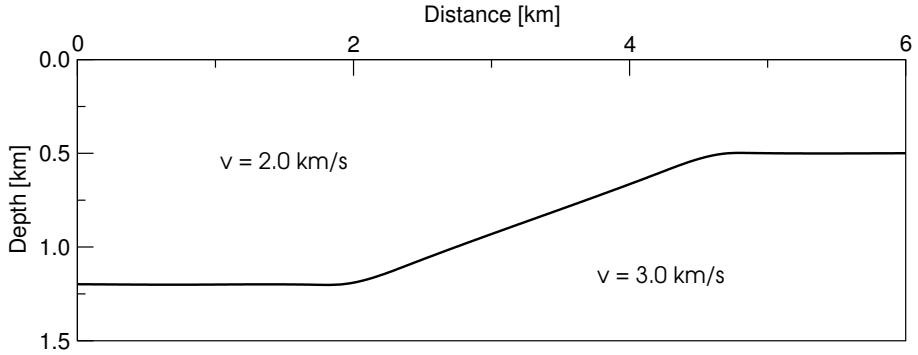

Figure 2: Model for the synthetic experiment. The two horizontal parts of the reflector are smoothly connected by a dipping reflector segment with a dip angle of 15 degrees.

Figure 4 shows the comparison of the optimal values of the velocity correction factor γ as obtained with formulas (19) and (20). The desired value of γ is 1.75 which is represented by white color. Note that the value for gamma is only meaningful at the position of the migrated reflector image. The values off this image are random values without any physical meaning. In the region of the horizontal parts of the migrated reflector image, we observe that both traveltime formulas determine the desired value of γ with reasonable accuracy. As can be seen at the dipping part of the reflector, the values for γ obtained from both formulas are not perfect. However, upon closer inspection, we see that the dip-corrected formula indeed provides somewhat better values.

The information about where these values are meaningful or not is contained in the corresponding coherence section. Figure 5 compares these sections for the two competing procedures. Both coherence sections are rather similar. This means that both formulas can be adjusted rather well to the data. The difference between the formulas lays in the quality of the obtained parameter values.

To extract the most meaningful values of the parameters, the maximum of each coherence trace has been picked. To discard outliers, a maximum was only accepted if it had at least 11 neighbours in a window of 23 which where higher than 3/4 of the maximum coherence value. The resulting curves of most reliable points also depicted in Figure 5.

The values of γ extracted from the sections in Figure 4 along these picking curves are compared in Figure 6. The values of γ obtained with Al-Yahya's formula (20) (red circles) quite accurately recover the true value of 1.75 at the horizontal parts of the reflector, but show a significant reduction at the dipping part. The values obtained with the dip-corrected formula (19) (green crosses) does a better job in this part, although suffering from more fluctuations.

The dip-corrected formula (19) provides, as an additional parameter, the optimal dip. As explained before, the attribute "optimal" is used in the sense that this is the parameter value that achieves best fit between the traveltime curve (19) and the position of the migrated reflector image. Figure 7 shows the resulting dip angles along the maximum coherence curve.

To better appreciate the quality of this parameter, the picked values have been smoothed with optimal splines. This technique is an optimized cubic spline approximation that has been developed by Biloti (2002). It differs from conventional spline interpolation in the fact that it detects, for a given number of control points, their best possible positions in a least-squares sense. We see from Figure 7 that the determined angle values recover the true reflector dip reasonably well. At the horizontal parts of the reflector, the values are close to zero, and at the dipping part, they come close to the true dip of 15 degrees.

Finally, the actual delivery of a migration-velocity analysis is the updated migration velocity field. The results of the processes based on the competing formulas are compared in Figure 8. After updating the original velocity field with the gamma values of Figure 6, the resulting velocity fields have been smoothed with optimal splines (Biloti, 2002). As can already be seen in Figure 8, the dip correction has indeed succeeded in providing a better updated velocity field in the area of the dipping reflector.

A more quantitative analysis is carried out in Figure 9. It shows the remaining velocity error along the reflector image after velocity updating. Note the diminished error in the region of the dipping reflector.

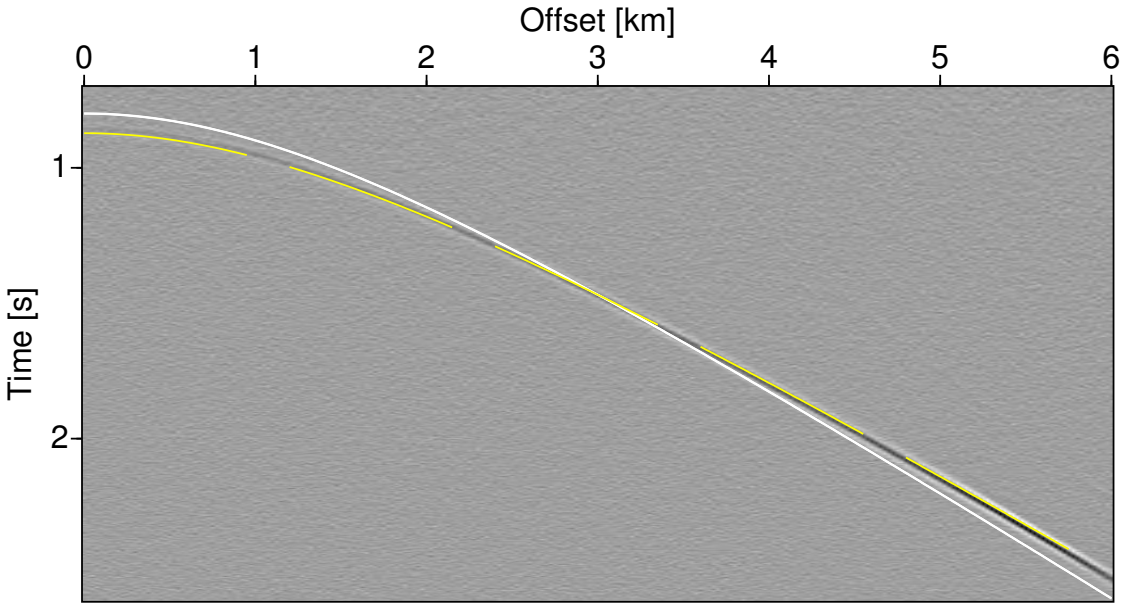

Figure 3: Image gather of the wrongly migrated data at a CMP position above the dipping part of the reflector. Also indicated are the theoretical predictions of the image position in this gather with (long dashed yellow curve) and without (solid white curve) dip correction as described by equation (19).

As a final test, the original data have been migrated with the updated velocity fields. The results are compared in Figure 10. While both methods image the horizontal parts of the reflector reasonably well, the dipping part is acceptably imaged only with the dip-corrected velocity.

CONCLUSIONS

In this paper, we have presented a dip correction to the coherence-based approach to migration velocity analysis (MVA) of Al-Yahya (1989). This approach is based on a coherence analyses along possible moveout curves in a migrated image gather for different values for the ratio (γ) between the migration and true medium velocities. The highest coherence determines the optimal values for this ratio, which can then be used to updated the migration velocity. This approach has the advantage that no picking is needed.

We have generalized the method of Al-Yahya (1989), which was restricted to horizontal reflectors, to dipping reflectors. In our new MVA technique, the reflector dip is treated as an additional search parameter, which is to be detected together with the velocity updating factor γ. Both parameters are searched-for simultaneously by the application of techniques that have been developed in connection with the common-reflection-surface (CRS) stack (Biloti et al., 2002). Like for that method, the search is carried out by determining trial curves as a function of the search parameters and stacking the migrated data along these curves. The highest coherence determines the best-fitting curve and thus the optimal, i.e., best-possible, parameter pair. In this way, estimates can be found not only for the velocity ratio γ but also for the reflector dip.

A numerical example has demonstrated that the additional search parameter can indeed be helpful for the analysis. Although curves described by Al-Yahya's original formula can be well fitted to the actual migration moveout, thus providing high coherence values, it turns out that the additional search parameter improves the estimates of the velocity ratio. In our example, the velocity was sufficiently well recovered in one step to produce a satisfactory final migrated image. With Al-Yahya's formula, one more iteration would have been necessary. Moreover, the recovery of the dip was also successful, providing reasonable estimates of the true reflector dip.

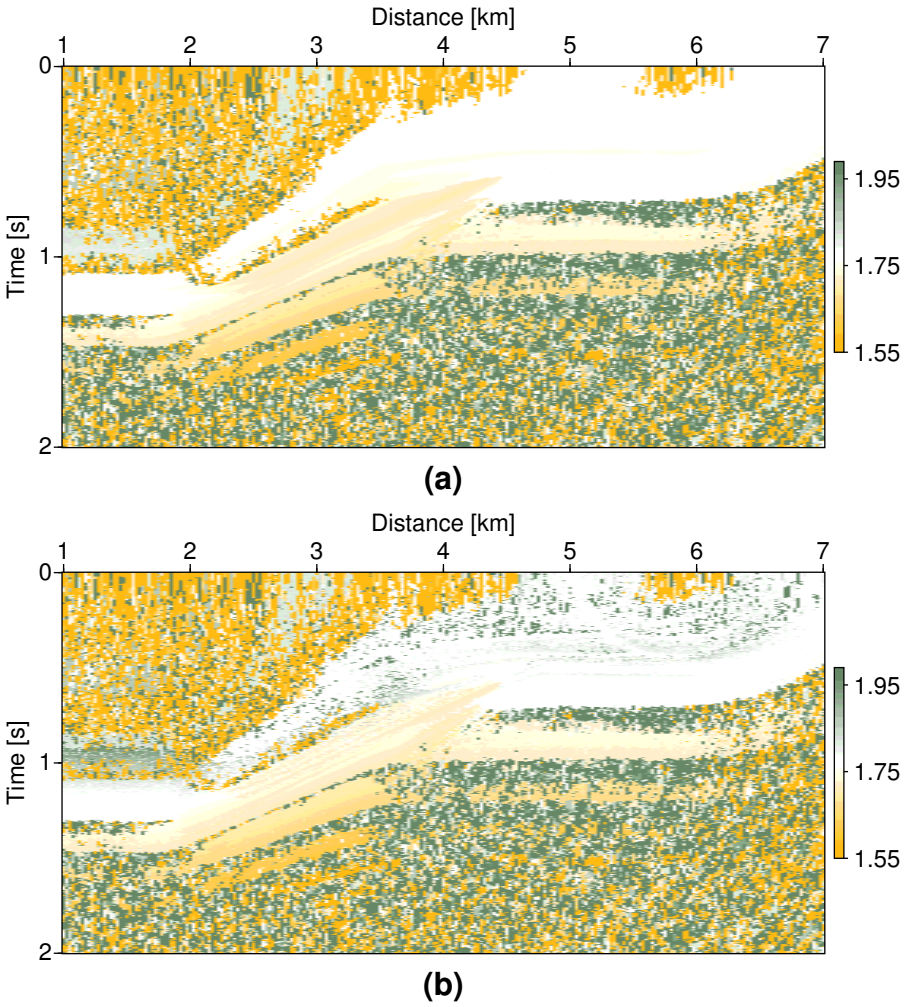

Figure 4: (a) Parameter γ as obtained from MVA using the Al-Yahya's formula (20). (b) Parameter γ as obtained from MVA using the the dip-corrected formula (19).

ACKNOWLEDGMENTS

The authors are grateful to Eduardo Filpo for making his modeling available. The most tedious algebraic manipulations of this paper have been carried out using Maple V Release 4. The research of this paper has been supported partially by the Research Foundation of the State of São Paulo (FAPESP), the National Research Council (CNPq) of Brazil, and the sponsors of the WIT Consortium Project.

REFERENCES

Al-Yahya, K. M. (1989). Velocity analysis by iterative profile migration. *Geophysics*, 54(06):718–729.

Audebert, F., Guillaume, P., Zhang, X., and Jones, I. (1998). CRP-Scan - solving 3D PreSDM velocity analysis with zero-offset. In *60th Ann. Internat. Mtg., EAGE*, pages Session:01-05. EAGE.

Billette, F., Etgen, J., and Rietveld, W. (2002). The key practical aspects of 3D tomography - data picking and model representation. In *64th Ann. Internat. Mtg., EAGE*, page B006. EAGE.

Billette, F., Le Begat, S., Podvin, P., and Lambare, G. (2003). Practical aspects and applications of 2D sterotomography. *Geophysics*, 68(3):1008–1021.

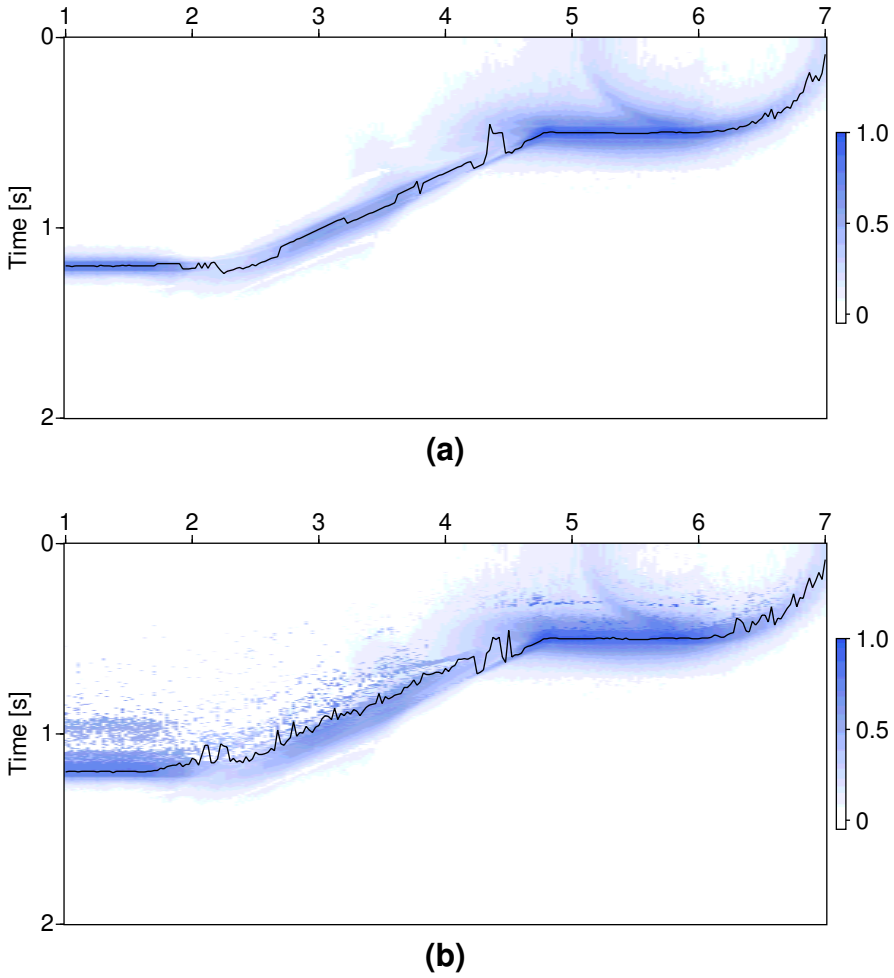

Figure 5: (a) Coherence as obtained from MVA using the Al-Yahya's formula (20). (b) Coherence as obtained from MVA using the the dip-corrected formula (19). Also shown in both parts is the path of maximum coherence.

Biloti, R. (2002). *Tomographic Inversion of the velocity model using multiparametric traveltimes*. PhD thesis, State University of Campinas, Brazil. In Portuguese.

Biloti, R., Santos, L. T., and Tygel, M. (2002). Multiparametric traveltime inversion. *Studia Geophysica et Geodaetica*, pages 177–192.

Biondi, B. and Sava, P. (1999). Wave-equation migration velocity analysis. In *69th Ann. Internat. Mtg., SEG*, pages 1723–1726. SEG.

Birgin, E. G., Biloti, R., Tygel, M., and Santos, L. T. (1999). Restricted optimization: a clue to a fast and accurate implementation of the common reflection surface stack method. *Journal of Applied Geophysics*, pages 143–155.

Bradford, J. H. and Sawyer, D. (2002). Depth characterization of shallow aquifers with seismic reflection, Part II–Prestack depth migration and field examples. *Geophysics*, 67(1):98–109.

Chauris, H., Noble, M. S., Lambare, G., and Podvin, P. (2002a). Migration velocity analysis from locally coherent events in 2-D laterally heterogeneous media, Part I: Theoretical aspects. *Geophysics*, 67(04):1202–1212.

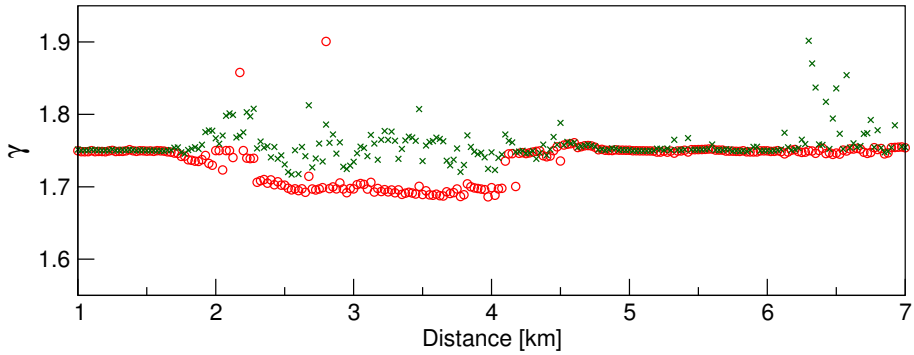

Figure 6: Values of γ as picked along the maximum coherence curves of Figure 5 (Al-Yahya: red circles, dip-corrected: green crosses).

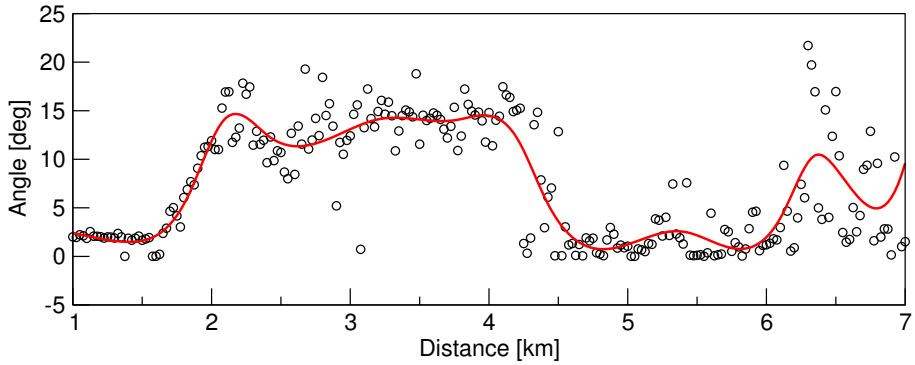

Figure 7: Dip angles along the maximum coherence curve (red circles) as obtained from MVA using the the dip-corrected formula (19). Also shown is the result of a smoothing of these data (solid line).

Chauris, H., Noble, M. S., Lambare, G., and Podvin, P. (2002b). Migration velocity analysis from locally coherent events in 2-D laterally heterogeneous media, Part II: Applications on synthetic and real data. *Geophysics*, 67(04):1213–1224.

Fowler, P. (1995). Migration velocity analysis by optimization: Linear theory. *SEP Report*, 44:1–20.

Kolda, T. G., Lewis, R. M., and Torczon, V. (2003). Optimization by direct search: New perspectives on some classical and modern methods. *SIAM Review*, 45(3):385–482.

Lafond, C. F. and Levander, A. R. (1993). Migration moveout analysis and depth focusing. *Geophysics*, 58(01):91–100.

Lee, W. B. and Zhang, L. (1992). Residual shot profile migration. *Geophysics*, 57(06):815–822.

Levin, F. (1971). Apparent velocity from dipping interface reflections. *Geophysics*, 36(3):510–516.

Liu, Z. (1997). An analytical approach to migration velocity analysis. *Geophysics*, 62(04):1238–1249.

Santos, L., Schleicher, J., Tygel, M., and Hubral, P. (2000). Seismic modeling by demigration. *Geophysics*, 65(4):1281–1289.

Symes, W. W. and Carazzone, J. J. (1991). Velocity inversion by differential semblance optimization. *Geophysics*, 56(05):654–663.

Woodward, M. J., Farmer, P., Nichols, D., and Charles, S. (1998). Automated 3-D tomographic velocity analysis of residual moveout in prestack depth migrated common image point gathers. In *68th Ann. Internat. Mtg., SEG*, pages 1218–1221. SEG.

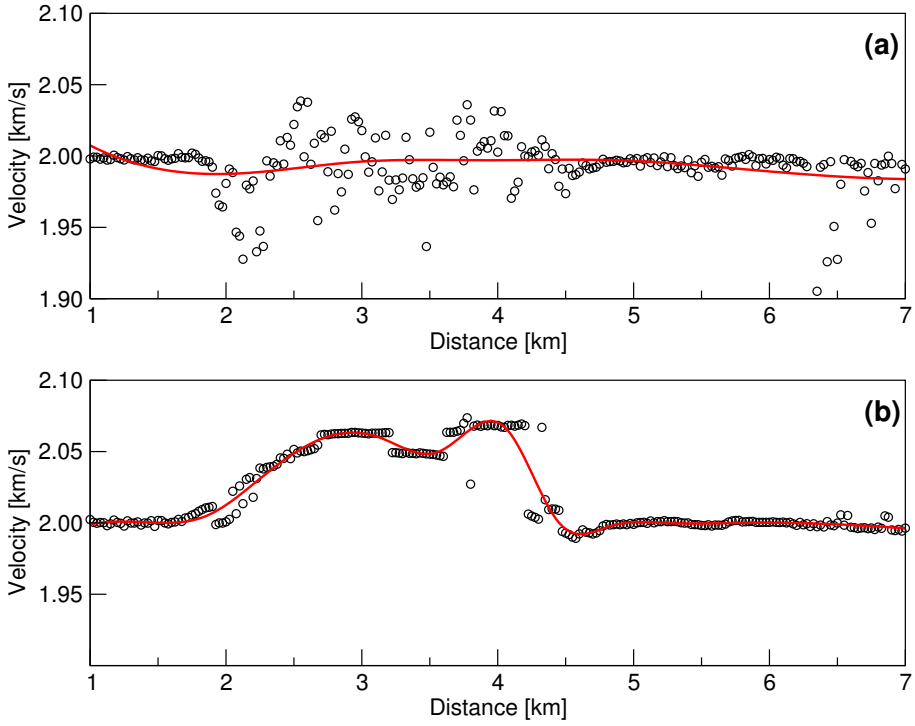

Figure 8: (a) Updated migration velocity as obtained from MVA using the Al-Yahya's formula (20) (point-to-point values: red circles, smoothed values: solid line). (b) Updated migration velocity as obtained from MVA using the the dip-corrected formula (19) (point-to-point values: red circles, smoothed values: solid line).

Yilmaz, O. and Chambers, R. E. (1984). Migration velocity analysis by wave-field extrapolation. *Geophysics*, 49(10):1664–1674.

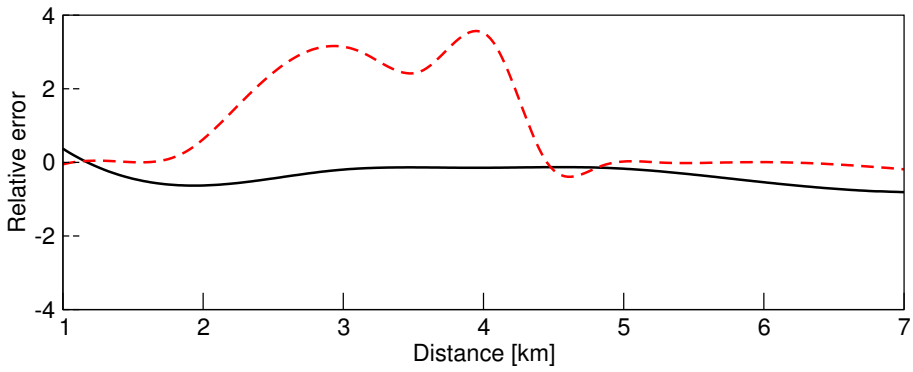

Figure 9: Error of updated migration velocity as obtained from MVA using the Al-Yahya's formula (20) (dashed red line) and using the the dip-corrected formula (19) (solid black line).

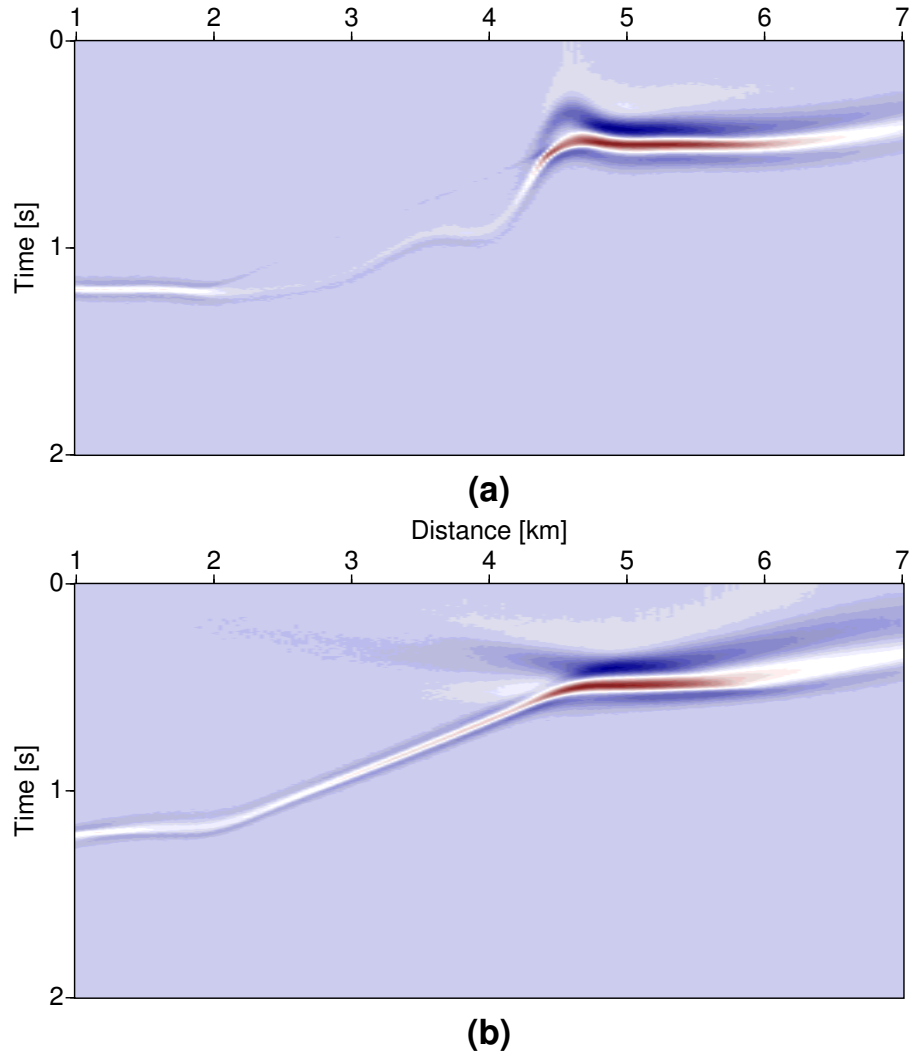

Figure 10: Stack of migrated images using (a) Al-Yahya's velocity update, (b) the dip-corrected velocity update.